Original Paper

Ophthalmic Research

Ophthalmic Res 2005;37:214–224
DOI: 10.1159/000086862

Received: October 19, 2004
Accepted: December 13, 2004
Published online: July 5, 2005

Dominant Optic Atrophy Caused by a Novel *OPA1* Splice Site Mutation (IVS20+1G→A) Associated with Intron Retention

Takaaki Hayashi Tamaki Gekka Satoshi Omoto Tomokazu Takeuchi
Kenji Kitahara

Department of Ophthalmology, Jikei University School of Medicine, Tokyo, Japan

Key Words
Optic atrophy · Autosomal dominant inheritance · Color vision defects · Splice site mutation · Intron retention · Premature termination codon · Nonsense-mediated mRNA decay

Abstract
Dominant optic atrophy (DOA) is the most common form of inherited primary optic neuropathy. The purpose of the current study was to report a novel *OPA1* splice site mutation and investigate the impact of the mutation on pre-mRNA splicing in a female proband and her father diagnosed with DOA. We evaluated visual acuity, retinal fundi and kinetic visual fields. Color vision phenotypes were determined using the Farnsworth Panel D-15 and the Farnsworth-Munsell 100-hue tests. All 28 coding exons of the *OPA1* gene were analyzed with polymerase chain reaction (PCR) amplification and direct sequencing. Total RNA extraction from white blood cells followed by reverse transcription-PCR (RT-PCR) was performed. We identified a novel heterozygous G to A mutation at position +1 of intron 20 (g.IVS20+1G→A) in both patients. RT-PCR analysis revealed that the first 25 bp from intron 20 plus exon 20 were spliced onto exon 21. No difference in expression of mutant and wild-type transcripts was found within the linear range of amplification. Clinically, both patients exhibited reduced visual acuities, pallor of optic discs, decreased sensitivities of central visual fields and blue-yellow color vision defects. Previously, only one mechanism (skipping of exon) of pre-mRNA splicing defects has been reported among *OPA1* splice site mutations. Our study demonstrates that the mechanism of intron retention is a novel type of pre-mRNA splicing defects. The mutant transcript with a premature termination codon is likely to encode a truncated protein, due to a translational frameshift (V672fsX675), that lacks 289 amino acids of the C-terminal end. Therefore, it is suggested that haploinsufficiency underlies DOA in the patients. However, we could not exclude the possibility that the truncated protein has a dominant negative activity because the mutant transcript is insusceptible to nonsense-mediated mRNA decay.

Introduction

Autosomal dominant optic atrophy (DOA) (MIM #165500), Kjer type [1], is the most common form of inherited primary optic neuropathy with a prevalence of 1:50,000 [2]. The disorder is characterized by a decreased visual acuity that occurs from childhood, temporal pallor of the optic discs, centrocecal scotoma and color vision defects [3–6]. Patients with DOA exhibit great intrafamilial phenotypic variations ranging from retention of good

KARGER

Fax +41 61 306 12 34
E-Mail karger@karger.ch
www.karger.com

0030–2414/05/0374–0214$22.00/0

Accessible online at:
www.karger.com/ore

Takaaki Hayashi, MD, PhD
Department of Ophthalmology, Jikei University School of Medicine
3-25-8, Nishi-shinbashi, Minato-ku, Tokyo 105-8461 (Japan)
Tel. +81 3 3433 1111, ext. 3581, Fax +81 3 5378 8828
E-Mail taka@jikei.ac.jp

visual acuity to legal blindness [7]. Generally, the visual prognosis is relatively good because of stable or slow progression of visual acuity loss [8, 9]. Histopathological studies using human donor eyes have shown diffuse atrophy of the ganglion cell layer that predominates in the central retina [10, 11]. Pattern electroretinograms show that patients with DOA have a reduced amplitude of the ganglion cell-specific component [9, 12, 13]. These findings support the hypothesis that the cause of DOA is due to the loss of function of the retinal ganglion cells.

Through linkage analysis, DOA has been linked to the telomeric region of chromosome 3q28-qter (OPA1) [14]. Subsequently, another locus has been mapped to chromosome 18q12.2–12.3 (OPA4) [15]. In European populations, a number of mutations responsible for DOA have been recently identified in a gene designated as *OPA1*, which is located in the OPA1 locus [16, 17]. These *OPA1* mutations included missense, nonsense, deletion, insertion and splice site mutations. Subsequently, *OPA1* mutations have also been found in Japanese patients with either DOA or bilateral optic atrophy [18–20]. The *OPA1* gene consists of 28 coding exons and encodes a 960 amino acid protein that belongs to a family of dynamin-related large guanosine triphosphatase proteins. Representative members include the yeast Mgm1/Msp1 [21, 22] and the human DRP1 [23], and these proteins are responsible for the maintenance of mitochondrial DNA (mtDNA). It has been demonstrated that the *OPA1* mRNA is ubiquitously expressed in human tissues, including the retina and white blood cells, consistent with the previously reported data on the mitochondrial localization [16, 17]. Abundant expression of the *OPA1* gene has also been observed in the retinal ganglion cell layer [24, 25].

Among splice site mutations in the *OPA1* gene, a total of seven mutations (six 5′ donor splice site and one 3′ acceptor splice site mutations) have been investigated at mRNA level using white blood cells in patients with DOA [24, 26–28]. Generally, mRNA splicing defects with splice site mutations have been classified into four categories, exon skipping, cryptic splice site activation, new splice site creation and intron retention [29]. Only one mechanism of exon skipping was causative among those seven splice site mutations in the *OPA1* gene. No other patterns of pre-mRNA splicing defects were reported.

In this study, we describe the clinical phenotypes in a Japanese family in which the female proband and her father were diagnosed with DOA, and identify a novel splice site mutation in the *OPA1* gene. In addition, we performed reverse transcription-polymerase chain reaction (RT-PCR) in order to investigate the impact of the mutation on pre-mRNA splicing, and we report on the findings for a new mechanism of pre-mRNA splicing defects in the *OPA1* gene.

Patients and Methods

The Ethics Review Board of Jikei University School of Medicine approved the research protocol. The protocol adhered to the tenets of the Declaration of Helsinki, and informed consent was obtained from all participants.

Clinical Studies

In a Japanese family (JU#0180) studied, we examined a female proband and her father who were diagnosed with DOA based on the presence of typical clinical features, which included bilaterally decreased visual acuity, abnormalities of central visual fields, pallor of the optic discs, color vision defects and familial occurrence with autosomal dominant inheritance. We performed ophthalmic examinations including best-corrected visual acuity (BCVA), Goldmann visual field tests, slit lamp and dilated fundus examinations. For evaluation of color vision, we used pseudoisochromatic plates, including the Ishihara test (38 plate edition) and standard pseudoisochromatic plates (SPP-2 for acquired color vision defects). Color vision was also evaluated using the Farnsworth Panel D-15 (Panel D-15) and the Farnsworth-Munsell (F-M) 100-hue tests. All color vision tests were performed monocularly for each eye. The patterns for the F-M 100-hue test were analyzed using a previously reported method [30]. Total error scores and orientation axes were calculated to determine the characteristics of the color vision defects. In addition, we examined the proband with a Nagel model I anomaloscope (Schmidt & Haensch, Berlin, Germany) for evaluation of red-green color vision defects. The size of the field of view was 2° in the anomaloscope.

Molecular Genetic Studies

OPA1 Mutation Screening

Genomic DNA was isolated from peripheral white blood cells using a Blood DNA Isolation Kit, PUREGENE (Gentra Systems, Minneapolis, Minn., USA), which was used as a template to amplify human *OPA1* genomic sequences. The sequences for all of the primers (Sigma-Genosys, Hokkaido, Japan) used in this study were obtained from a previous paper [31]. All coding exons (a total of 28 exons) of the *OPA1* gene were amplified by PCR. Additional exons (exons 4b and 5b) [26] were also analyzed. All PCR reagents, except for the primers, were supplied by Takara-Bio (Shiga, Japan). The PCR amplifications were performed in a DNA Thermal Cycler (PTC-200, MJ Research, Waltham, Mass., USA), analyzed on 2% agarose gels and visualized by ethidium bromide. Then, the PCR products were purified with a QIAquick PCR Purification Kit (Qiagen K.K., Tokyo, Japan) and were used as templates for sequencing. Both strands were analyzed on an automated sequencer (ABI Prism 3700 DNA Analyzer, Applied Biosystems, Tokyo, Japan) using a BigDye Terminator kit v3.1 (Applied Biosystems). Nomenclature for the description of sequence variations is based on the recommendations [32, 33].

Restriction Enzyme Analysis

For screening the g.IVS20+1G→A mutation that was found in the proband, a method of PCR-restriction fragment length polymorphism (PCR-RFLP) was used. A 253-bp fragment of exon 20 containing the 5′ splice donor site of intron 20 was amplified by PCR using primers OPA1-20bF (5′-AGGAAATCCTTCAACAATCTTTG-3′) and OPA1-20bR (5′-AGGCTGTGATGGGAATAAAATC-3′). The PCR conditions were as follows: 1 min of denaturation at 94°C followed by 38 cycles of denaturation at 96°C for 10 s, annealing and polymerization at 62°C for 30 s and a final polymerization step of 5 min at 72°C. The PCR products were digested with a restriction endonuclease, *Mnl*I (New England Biolabs, Beverly, Mass., USA), and electrophoresed on 3% agarose or 10% polyacrylamide gels. The only wild-type allele was cleaved with the enzyme, resulting in 154- and 99-bp fragments.

Mutation Screening of mtDNA

Three primary mtDNA mutations (at nucleotide positions 3460, 11778 and 14484) associated with Leber's hereditary optic neuropathy (LHON) were screened by PCR amplification followed by sequencing. It has been demonstrated that these three primary mtDNA mutations account for nearly 100% of the causative mutations for LHON in the Japanese population [34]. The nucleotide sequences of the PCR primers have been previously reported [34].

Reverse Transcription-PCR

Total RNA was extracted from white blood cells (10 ml of peripheral blood) using a TRIzol reagent (Invitrogen, Tokyo, Japan) and dissolved in 30 μl of DEPC-treated water. For first-strand cDNA synthesis, reverse transcription was performed in a total volume of 10 μl using 50–100 ng of total RNA, a random hexamer and SuperScript III reverse transcriptase (Invitrogen) according to the manufacturer's protocol. The cDNA was treated with RNaseH before use in PCR amplification. PCR was performed in a total volume of 25 μl using 0.5 μl of cDNA, dNTPs (200 μ*M*), 1× Ex-PCR buffer (2 m*M* Mg^{2+} plus), one unit of Ex*Taq* polymerase (Takara) and two primer pairs (0.16 μ*M*), OPA1-E17aF (a sense primer in exon 17, 5′-ATGGTACGAGAGTCTGTTGAAC-3′) and OPA1-E23aR (an antisense primer in exon 23, 5′-GGTCCGATTCTTCCAGTATAACC-3′), and OPA1-E19F (a sense primer in exon 19, 5′-GCCAGGTTACACCAAAACATTG-3′) and OPA1-E21bR (an antisense primer in exon 21, 5′-TTGTAGGGTCTCCCAAGCAAC-3′). Those PCR product sizes for wild type are 684 bp (OPA1-E17aF and OPA1-E23aR) and 209 bp (OPA1-E19F and OPA1-E21bR). The PCR conditions were as follows: 1 min of denaturation at 94°C followed by 38 cycles of denaturation at 96°C for 10 s, annealing and polymerization at 64°C for 1 min (OPA1-E17aF and OPA1-E23aR) or 62°C for 30 s (OPA1-E19F and OPA1-E21bR), and a final polymerization step of 5 min at 72°C. In a pilot study, we found that the linear range of amplification (OPA1-E19F and OPA1-E21bR) was between 25 and 30 cycles. RT-PCR was performed with 25, 27, 28, 29 and 30 PCR cycles.

Cloning of RT-PCR Products

The RT-PCR products that were obtained with the primer pair (OPA1-E17aF and OPA1-E23aR) were purified using QIAquick PCR Purification Kit (Qiagen). TA cloning was performed using a TOPO TA Cloning Kit (Invitrogen) with 2 μl of the PCR products and a pCR2.1-TOPO vector according to the manufacturer's protocol. For transformation, 2 μl of the cloning product and OneShot chemically competent *Escherichia coli* (Invitrogen) were used. The transformation reaction was spread onto LB plates containing 50 μg/ml ampicillin and X-Gal (β5-bromo-4-chloro-3-indolyl-β-*D*-galactopyranoside; Promega). After an overnight incubation at 37°C, white colonies were picked up and miniprep was performed using a QIAprep Spin Miniprep Kit (Qiagen). Each clone was then sequenced with the OPA1-E18aF primer (5′-GTTTTAACCTTGAAACTGAATGG-3′) in exon 18.

Results

Mutation Detection in the OPA1 *Gene*

All coding exons and exon/intron boundaries in the *OPA1* gene were screened for mutations by sequencing of the PCR-amplified products from genomic DNA. The proband (patient II-2, JU#0180) was found to have a heterozygous G to A mutation at position +1 of intron 20 (g.IVS20+1G→A) (fig. 1A) that is likely to have abolished the 5′ donor splice site. No other sequence variants were detected by direct sequencing of these PCR products except for the homozygous g.IVS4–19T→C and g.IVS26+25T→A variants, which were also found in normal controls. Mutation analysis was performed in her family using the PCR-RFLP approach, and revealed that the affected father (patient I-1) was also heterozygous for the g.IVS20+1G→A mutation whose allele of the PCR product (OPA1-20bF and OPA1-20bR) was uncut with the enzyme *Mnl*I, whereas the asymptomatic sister (II-1) and mother (I-2) did not carry the mutation (g.IVS20+1G→A) (fig. 1B). The mutation was not detected in 110 individuals without ocular abnormalities. The mtDNA mutations associated with LHON were not detected in both patients. Also, the male to female transmission could exclude inherited mitochondrial diseases such as LHON.

OPA1 *mRNA Analysis*

The *OPA1* gene is ubiquitously expressed in various tissues [16, 17], including the white blood cells [24]. Northern blot analysis showed the highest transcript level was detected in the retina [16]. To investigate the impact of the splice donor site mutation (g.IVS20+1G→A) on pre-mRNA splicing, we analyzed *OPA1* transcripts expressed in the white blood cells from patient II-2 and her unaffected mother (I-2). Only approximately 700-bp cDNA fragments extending from exons 17-23 (corresponding to sizes, 684 bp, from the wild-type alleles) from the RT-PCR (OPA1-E17aF and OPA1-E23aR primers)

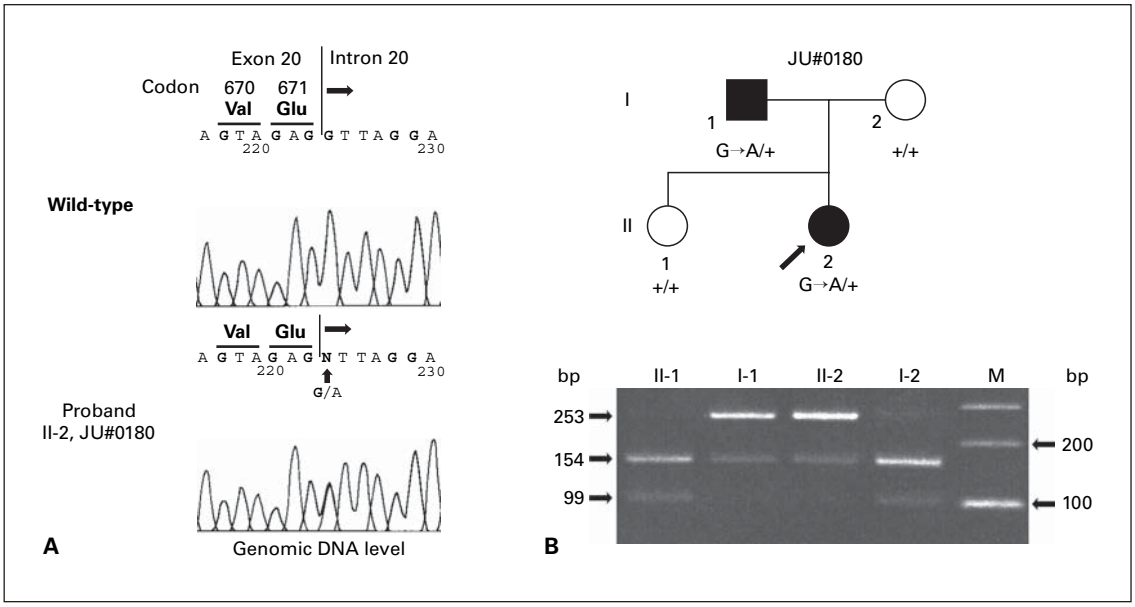

Fig. 1. Genomic DNA analysis of the *OPA1* gene in the family JU#0180. **A** Sequences of the wild-type allele and the mutant allele (patient II-2). In the mutant allele, a heterozygous G to A mutation, indicated by a vertical arrow, is shown at the +1 position of intron 20 (g.IVS20+1G→A) in the patient. **B** PCR-RFLP analysis of the mutation in the family. The PCR product (253 bp) harboring the wild-type allele is cleaved with the restriction enzyme *Mnl*I, resulting in 154- and 99-bp fragments. Unaffected subjects (sister, II-1, and mother, I-2) have only the wild-type alleles, while each of the affected subjects (I-1 or II-2) are heterozygous for the G to A mutation and have an uncut band (253 bp) from the mutant allele as well as the wild-type allele. M indicates a 100-bp ladder molecular weight marker.

were detected in both subjects, and there was no band around 518 bp, which should be detected if skipping of exon 20 had occurred. To separate mutant transcripts from wild-type transcripts, the RT-PCR products were TA-cloned as described in the methods section. A total of 20 TA clones from patient II-2 were sequenced to verify inserts, and these showed only two types of sequence variants. These included 14 clones that were wild-type transcripts and 6 clones that were mutant transcripts that had the first 25 bp from intron 20 plus exon 20 spliced onto exon 21 (fig. 2A, B), which would yield a truncated protein (p.V672fsX675) with a premature termination codon (PTC) due to a translational frameshift (fig. 2A). Therefore, we comprehended that the RT-PCR products had both wild-type and mutant transcripts, corresponding to 684- and 709-bp fragments. In the mother, TA clones only from the wild-type transcripts were observed. To distinguish the wild-type from the mutant transcripts on a gel without cloning, we performed RT-PCR using OPA1-E19F and OPA1-E21bR primers. This analysis revealed that patient II-2 had both wild-type (209 bp) and mutant (234 bp) transcripts, while her unaffected mother (I-2) had only the wild-type (209 bp) transcript (fig. 2C). The RT-PCR result within the linear range of amplification showed that both mutant and wild-type transcripts were initially detected in 27 or 28 PCR cycles in patient II-2 (fig. 3).

Clinical Characteristics

Patient II-2

Patient II-2 (the proband) was a 24-year-old female who was referred to our department for evaluation of color vision defects. At the time of her first visit to our hospital, BCVA was 0.9 in the right eye with –2.75 sphere, –0.50 cylinder 60° and 0.8 in the left eye with –2.75 sphere, –0.50 cylinder 150°. Her visual acuity was good, and she had previously passed all vision-screening examinations that used the Ishihara test during the entire time she attended elementary school (6–12 years old). A Goldmann kinetic visual field test showed a constriction to the I/2e test light in the right eye, but neither midpe-

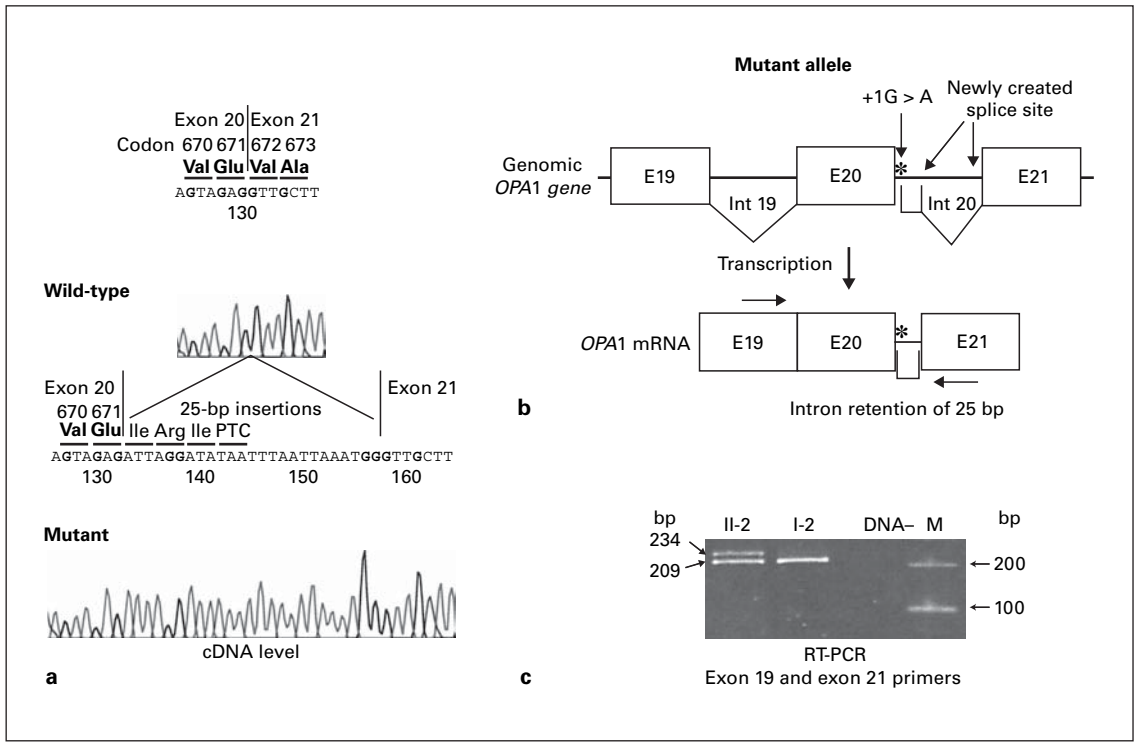

Fig. 2. *OPA1* cDNA analysis in the family JU#0180. **A** Sequences of the wild-type (normal splicing) and mutant (aberrant splicing) cDNAs from white blood cells. The intron 20 is normally spliced out (wild type), while the cDNA sequence from the mutant transcript shows retention of the first 25 bp of intron 20 (mutant), which is expressed as an abnormal exon. The PTC is located on 16 bp upstream of the junction between the abnormal exon and exon 21. **B** Diagram showing abnormal pre-mRNA splicing by intron retention. The first 25 bp from intron 20 plus exon 20 are spliced onto exon 21. **C** Gel electrophoresis of the RT-PCR products (OPA1-E19F and OPA1-E21bR) from patient II-2 and the unaffected mother (I-2). The mother has only a 209-bp product, while the patient has a 234-bp product with intron retention of the 25-bp as well as the 209-bp product. Asterisks indicate position of the +1G→A mutation.

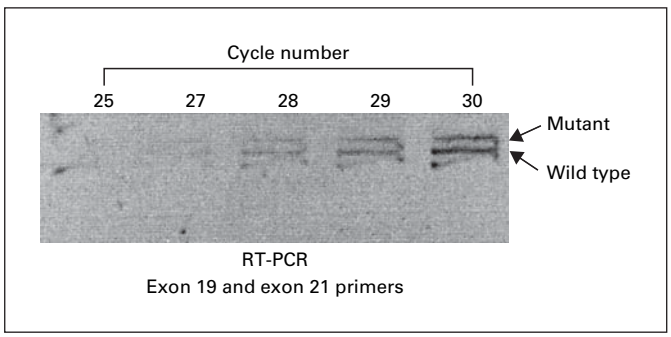

Fig. 3. Analysis of RT-PCR within the linear range of amplification in patient II-2. RT-PCR (OPA1-E19F and OPA1-E21bR) is performed with 25, 27, 28, 29 and 30 cycles. Both mutant and wild-type transcripts were initially detected in 27 or 28 PCR cycles.

ripheral scotomas nor peripheral visual field constrictions in both eyes (fig. 4A). There was no relative afferent pupillary defect. No specific findings were observed on examination of the anterior segments. Fundus examination showed temporal pallor of the optic discs with a gray crescent and temporal peripapillary atrophy in both eyes (fig. 5A, B), but no maculopathy was seen. In color vision tests, she identified only the first plate on the Ishihara test and no plates on the SPP-2 test that were used to evaluate each eye. However, the Panel D-15 showed that she had no errors in the right eye and minor errors in the left eye (fig. 6). In the F-M 100-hue tests (fig. 6), the square roots calculated from the total error scores were 14.3 (right eye) and 17.2 (left eye). The average for a group of 20- to 29-year-olds with normal color vision and good visual acuity has been reported to be 6.5–7.5 [35, 36]. We have previously reported 42 cases with acquired blue-yellow color

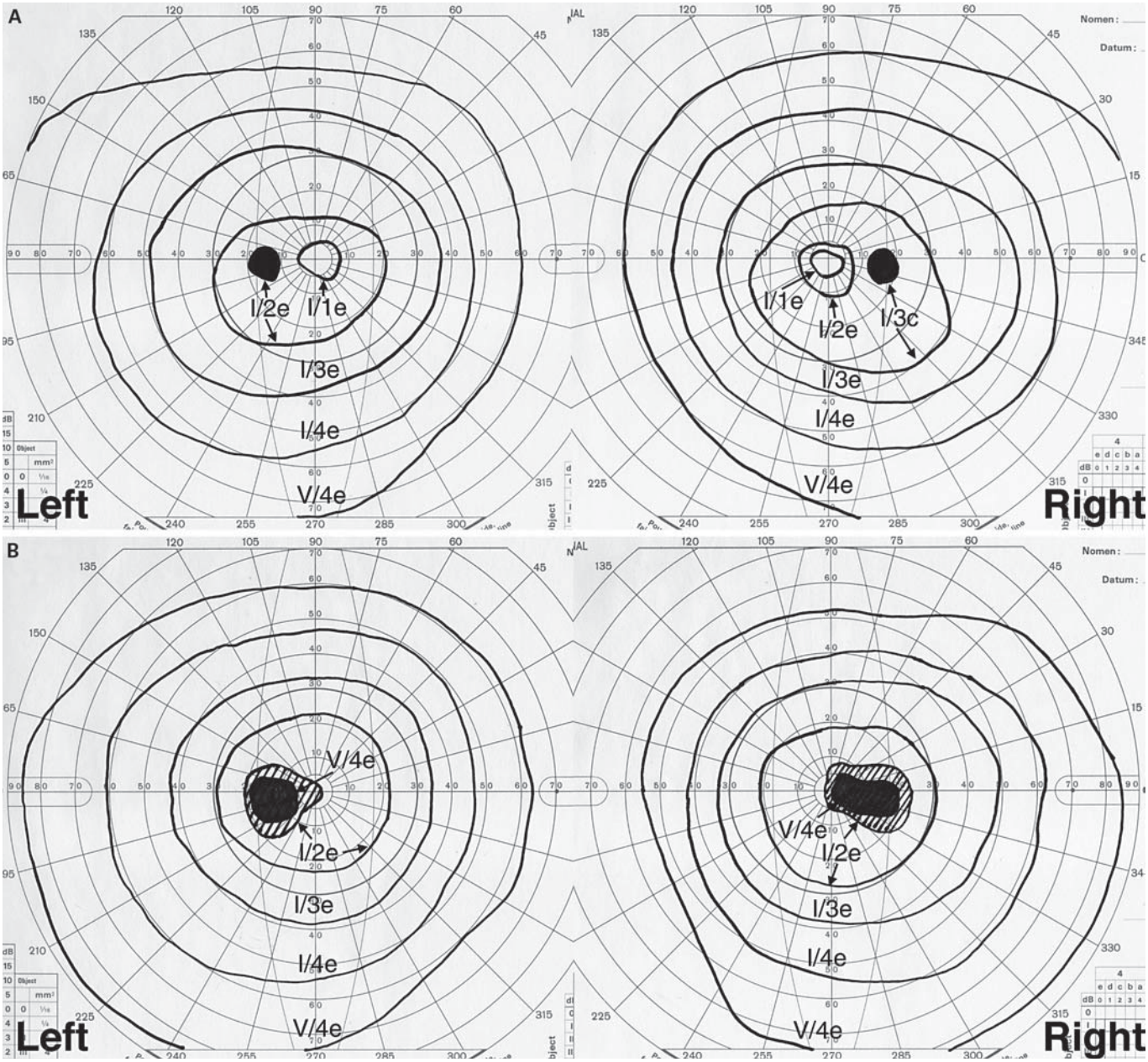

Fig. 4. Goldmann kinetic visual field tests. **A** A constriction to the I/2e test light are observed in the right eye of patient II-2. Midperipheral and peripheral isopters are intact in both eyes. **B** Bilateral centrocecal scotomas (I/2e test lights) are observed in the affected father (I-1), although the midperipheral and peripheral isopters are intact in both eyes.

vision defects in whom the range of the orientation axes was within –0.620 to 6.758 [30]. The orientation axes of the patient were 42.17 (right eye) and 3.65 (left eye), indicating that she had blue-yellow defects in the left eye and color vision defects without any certain axis in the right eye. The anomaloscope examination for red-green color vision defects showed that the Rayleigh equation was 39–43 in the right eye. The matching range was slightly enlarged as compared with the 41.2 mean value that has been reported for 72 Japanese individuals with normal color vision [37].

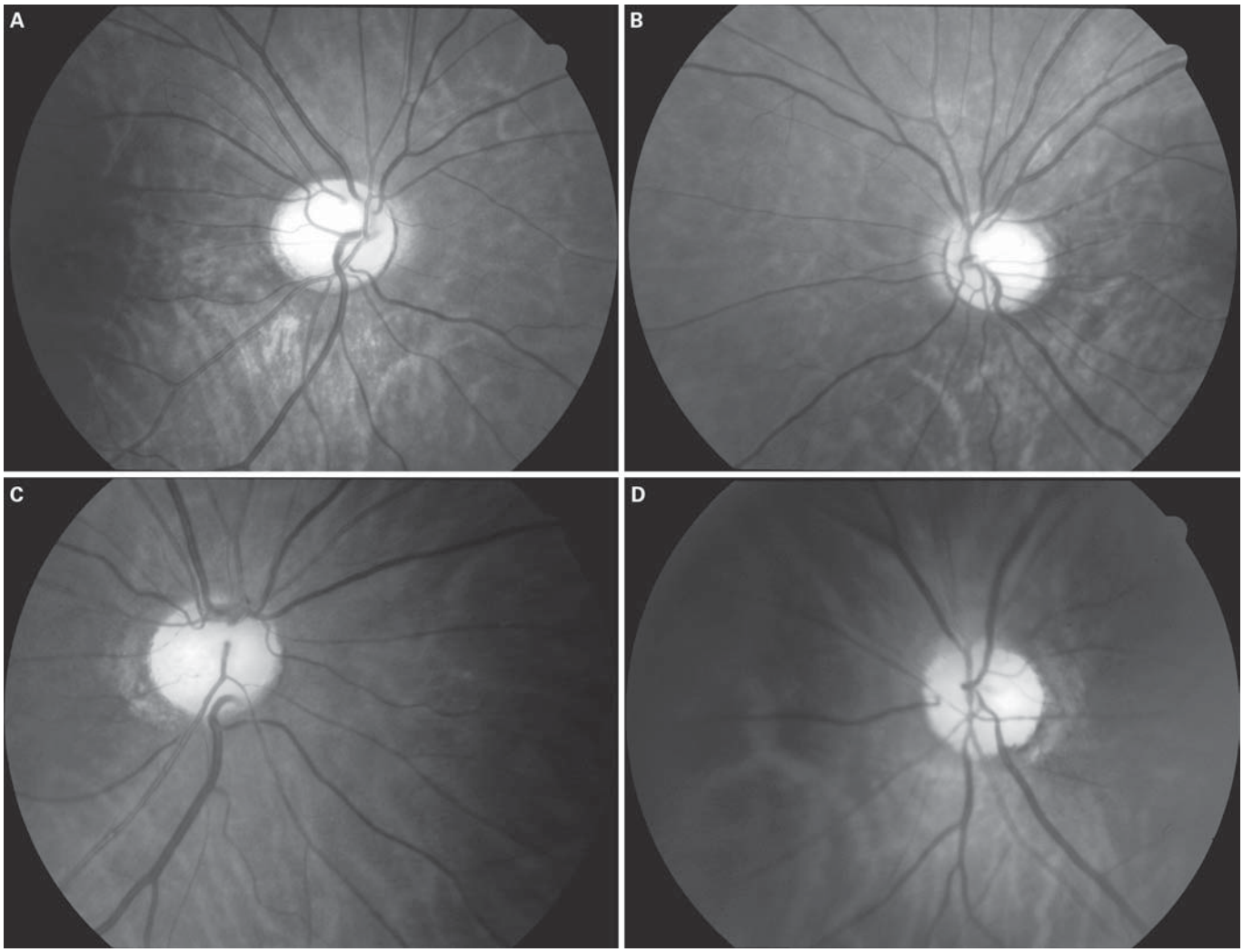

Fig. 5. Color photographs of the optic discs. **A** Right fundus of patient II-2. **B** Left fundus of patient II-2. The photographs show temporal pallor of the optic discs with a gray crescent and temporal peripapillary atrophy in both eyes. **C** Right fundus of the affected father (I-1). **D** Left fundus of the father. The photographs show diffuse optic disc pallor in the right eye and temporal optic disc pallor in the left eye. Temporal peripapillary atrophy is seen in both eyes.

Patient I-1

The 62-year-old father of the proband had had decreased visual acuity since adolescence. BCVA was 0.1 in both eyes. Refractions were +0.50 sphere, –1.00 cylinder 100° in the right eye and –2.75 sphere, +0.50 sphere, –1.00 cylinder 90° in the left eye. In the past, he had never failed vision-screening examinations (visual acuity and the Ishihara test) at least during the period of attendance at elementary school. Therefore, the acuity loss had been progressive over patient's lifetime. A Goldmann visual field test showed bilateral centrocecal scotomas (I/2e test lights) in both eyes (fig. 4B). There was no relative afferent pupillary defect. No specific findings were observed on examination of the anterior segments except for senile cataract in both eyes. Fundus examination showed diffuse optic disc pallor in the right eye and temporal optic disc pallor in the left eye (fig. 5A, B). Temporal peripapillary atrophy was seen, but there was no maculopathy in either eye. In color vision tests, he identified only the first plate on the Ishihara test and no plates on the SPP-2 test in both eyes. The Panel D-15 showed that the confusion pattern was consistent with the tritan axis in each eye (fig.

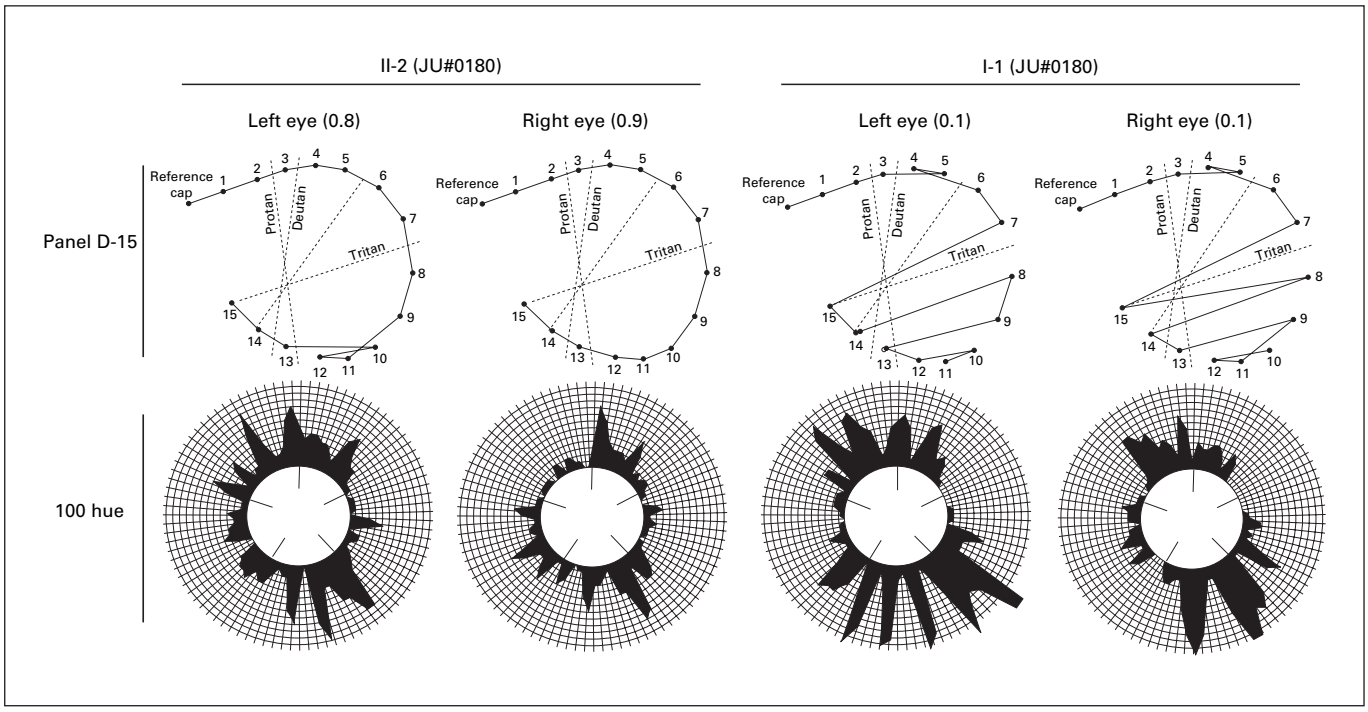

Fig. 6. The Panel D-15 and F-M 100-hue tests. In patient II-2, the Panel D-15 shows that she has minor errors in the left eye but no errors in the right eye. The F-M 100-hue tests show a blue-yellow defect in the left eye and a color vision defect without any certain axis in the right eye. In the affected father (I-1), the Panel D-15 shows that the confusion pattern is consistent with tritan (blue-yellow defect) axis in each eye. Also, the F-M 100-hue test shows blue-yellow axis in each eye. BCVA is indicated in the parentheses.

6). The F-M 100-hue tests (fig. 6) revealed that the total error scores were 16.6 (right eye) and 19.5 (left eye). The average in a group of 60- to 69-year-olds with normal color vision and good visual acuity has been reported to be 10.0–11.0 [35, 36]. The orientation axes for the father were 6.12 (right eye) and 5.40 (left eye), indicating that he has blue-yellow color vision defects in both eyes. Therefore, it was assumed that there was a progressive deterioration of color vision.

Discussion

Our molecular genetic study demonstrates that the DOA in the Japanese family (JU#0180) was caused by a novel 5′ donor splice site mutation (g.IVS20+1G→A) in the *OPA1* gene. It is estimated that up to 15% of all point mutations causing human genetic disease result in mRNA splicing defects [38]. Database analysis of aberrant splicing revealed that the frequency of the 5′ donor splice site mutations is higher than that of the 3′ acceptor splice site mutations [29]. Generally, splicing defects have been classified into four categories, exon skipping, cryptic splice site activation, intron retention and new splice site creation [29]. Among these patterns, exon skipping is the most frequent, while intron retention is less frequent.

A number of mutations in the *OPA1* gene have been found in patients with DOA [16, 17, 24, 31]. Although eighteen splice site mutations have been reported so far [17, 24, 26–28, 31], it is difficult to predict which of the splice site mutations will result in which of the four splicing defect patterns. It has been reported that the *OPA1* mRNA is expressed in white blood cells [24]. This has facilitated determination of the type of pre-mRNA splicing defects that occur in the *OPA1* transcripts. Only seven of the splice site mutations in the *OPA1* gene, g.IVS8+5G→A [26, 27], c.984G→A (the last nucleotide of exon 9) [26], c.983A→G [28], g.IVS9–1G→A [26], g.IVS10+3A→C [24], g.IVS12+1G→A [27] and c.2707G→C (the last nucleotide of exon 26) [26] have previously been investigated at the mRNA level in white blood cells, and the results indicated that there was skip-

ping of exons 8, 9, 9, 10, 10, 12 and 26, respectively. Thus, only the mechanism of exon skipping was causative of the splice site mutations that were seen in the *OPA1* gene.

In the RT-PCR and cloning analysis, we found that the splice site mutation (g.IVS20+1G→A) results in the retention of the first 25 bp of intron 20 with a newly created 5′ donor splice site (IVS20+26,27GT) (fig. 2A, B). It is predicted that this mutation causes a truncated protein (p.V672fsX675) with the PTC (fig. 2A) that lacks 289 amino acids of the C-terminal. This mechanism of intron retention (mRNA expression of intronic 25 bp as an abnormal exon) is a novel type of pre-mRNA splicing defects caused by splice site mutations in the *OPA1* gene.

Next, we addressed to define whether the mutant (PTC-containing) transcript undergoes nonsense-mediated mRNA decay (NMD) that is a general mechanism for clearing of RNA molecules containing PTCs [39]. NMD generally degrades mRNAs that have a splicing-generated exon-exon junction that is located more than 50–55 nucleotides downstream of the translation termination codon [40, 41]. Within the linear range of amplification, both mutant and wild-type transcripts were initially detected in 27 or 28 cycles of PCR (fig. 3). The result indicates that the mutant transcript is insusceptible to NMD. The reason may be due to the fact that the PTC is located on 16 bp upstream of the junction between the abnormal exon and exon 21 (fig. 2A). The expressed truncated OPA1 protein lacks a part of the dynamin central region and the coiled-coil formation in the C-terminal end [26, 42]. Although the functions of these domains are not well understood, the truncated protein must have a loss of function of the C-terminus, suggesting that haplotype insufficiency underlies the DOA in our patients.

Regarding the phenotype of color vision, a blue-yellow color vision defect occurs as the most common color vision defect in DOA [1, 43]. This defect can be observed even in cases that have minimal visual acuity loss [5]. In our study, although patient II-2 passed the Panel D-15 in both eyes, the F-M 100-hue test results revealed that there was a blue-yellow defect in the left eye and an unclassified color vision defect in the right eye, even though she had good visual acuity. Our findings support that the F-M 100-hue test is the most sensitive for the evaluation of acquired color vision defects as previously studied [4, 5, 43, 44]. In her father, blue-yellow defects were detected even in the Panel D-15 (fig. 6), suggesting that he has more severe color vision defects compared with patient II-2. When patient II-2 was in elementary school, she passed all her Ishihara tests and had a better visual acuity. But at the age of 24, she could only identify the first plate of the Ishihara test. Thus, these findings indicate that her color vision had been defective and that her visual acuity had slightly decreased since the time of elementary school. Also, her father's visual acuity loss and color vision defects had been progressive over his lifetime by his history. As it has been reported that better color vision is associated with a younger age and better visual acuity [9], both patients had better color vision and visual acuity when they were younger. Therefore, the history of our patients suggests that their color vision phenotypes were not stationary. On the contrary, they had been progressively deteriorating and eventually became blue-yellow color vision defects with decreased visual acuity.

In many cases, such as patient I-1, defective patterns of visual fields have shown centrocecal scotomas (fig. 4B). The data support the fact that the ganglion cells and their unmyelinated axons that constitute the papillomacular bundle are preferentially impaired. This is consistent with previous reports on the histopathological findings for the retina [10, 11] where the loss of ganglion cells, especially in the perifoveal macula, has been noted. These findings suggest that the papillomacular bundle is particularly susceptible in patients with DOA. In contrast, peripheral isopters in the Goldmann visual field tests were generally intact [4, 45], as seen in both patients (fig. 4). The *OPA1* is abundantly expressed in the retinal ganglion cell layer and is localized on the mitochondria [17, 24, 25]. A recent study using human donor eyes demonstrated that varicosities of the intraretinal ganglion cell axons are rich in mitochondria [46]. Therefore, the papillomacular bundle may contain more abundant varicosities than the ganglion cells and their unmyelinated axons that are located on the midperipheral and peripheral retina. Since in our patients the truncated *OPA1* protein that lacks the 289 amino acids of the C-terminus must have a loss of function, the contribution from a normal single allele may be insufficient to maintain the mitochondrial function in each of the ganglion cells that constitute the papillomacular bundle. However, as both patients had normal peripheral visual fields (fig. 4), the expression of only the normal single allele must be sufficient for the maintenance of each of the ganglion cells and their axons that are not part of the papillomacular bundle. Recent studies showed that culture cells deleted or down-regulated of the OPA1 were extremely sensitive to exogenous apoptosis induction and some died spontaneously, indicating that the OPA1 may function normally as an anti-apoptotic protein [47–49]. Therefore, loss of ganglion cells of the central retina in DOA may be caused by apoptosis.

In conclusion, we have characterized a novel 5′ donor splice site mutation in intron 20 (g.IVS20+1G→A) of the *OPA1* gene, and showed with RT-PCR analysis that the first 25 bp from intron 20 plus exon 20 are spliced onto exon 21. Among splice site mutations in the *OPA1* gene, only one mechanism (skipping of exon) of pre-mRNA splicing defects has been previously reported [24, 26, 27]. Our study demonstrated that the mechanism of intron retention is a novel type of pre-mRNA splicing defects in the *OPA1* gene, and the mutant transcript is insusceptible to NMD. The truncated protein caused by the mutation must lack function of the C-terminus, suggesting that haploinsufficiency underlies DOA in the patients, compatible with interpretation of the visual-field findings. However, we could not exclude the possibility that the truncated protein has a dominant negative activity because of insusceptibility to NMD. Through the clinical course of color vision phenotypes, it was ascertained that the color vision defects in our patients were not stationary but progressive, and over the lifetime of the patients eventually became blue-yellow (tritan) defects. Due to the low number of patients in the family, future follow-up of them is necessary for further understanding of the long-term history of DOA with the g.IVS20+1G→A mutation in the *OPA1* gene.

Acknowledgements

The authors thank the patients for their participation. This work was supported in part by grants from the Ministry of Education, Culture, Sports, Science and Technology of Japan (No. 16791073, T.H.), and from the Bio-Venture foundation (Hashira III), Institute of DNA Medicine, Jikei University School of Medicine (T.H. and K.K.).

References

1 Kjer P: Infantile optic atrophy with dominant mode of inheritance: A clinical and genetic study of 19 Danish families. Acta Ophthalmol (Copenh) 1959;164:1–147.
2 Lyle WM: Genetic Risks: A Reference for Eye Care Practitioners. Waterloo, University of Waterloo Press, 1990.
3 Caldwell JB, Howard RO, Riggs LA: Dominant juvenile optic atrophy. A study in two families and review of hereditary disease in childhood. Arch Ophthalmol 1971;85:133–147.
4 Kline LB, Glaser JS: Dominant optic atrophy. The clinical profile. Arch Ophthalmol 1979;97:1680–1686.
5 Hoyt CS: Autosomal dominant optic atrophy. A spectrum of disability. Ophthalmology 1980;87:245–251.
6 Jaeger W: Diagnosis of dominant infantile optic atrophy in early childhood. Ophthalmic Paediatr Genet 1988;9:7–11.
7 Votruba M, Moore AT, Bhattacharya SS: Clinical features, molecular genetics, and pathophysiology of dominant optic atrophy. J Med Genet 1998;35:793–800.
8 Eliott D, Traboulsi EI, Maumenee IH: Visual prognosis in autosomal dominant optic atrophy (Kjer type). Am J Ophthalmol 1993;115:360–367.
9 Votruba M, Fitzke FW, Holder GE, Carter A, Bhattacharya SS, Moore AT: Clinical features in affected individuals from 21 pedigrees with dominant optic atrophy. Arch Ophthalmol 1998;116:351–358.
10 Johnston PB, Gaster RN, Smith VC, Tripathi RC: A clinicopathologic study of autosomal dominant optic atrophy. Am J Ophthalmol 1979;88:868–875.
11 Kjer P, Jensen OA, Klinken L: Histopathology of eye, optic nerve and brain in a case of dominant optic atrophy. Acta Ophthalmol (Copenh) 1983;61:300–312.
12 Berninger TA, Jaeger W, Krastel H: Electrophysiology and colour perimetry in dominant infantile optic atrophy. Br J Ophthalmol 1991;75:49–52.
13 Holder GE, Votruba M, Carter AC, Bhattacharya SS, Fitzke FW, Moore AT: Electrophysiological findings in dominant optic atrophy (DOA) linking to the OPA1 locus on chromosome 3q 28-qter. Doc Ophthalmol 1998;95:217–228.
14 Eiberg H, Kjer B, Kjer P, Rosenberg T: Dominant optic atrophy (OPA1) mapped to chromosome 3q region. I. Linkage analysis. Hum Mol Genet 1994;3:977–980.
15 Kerrison JB, Arnould VJ, Ferraz Sallum JM, Vagefi MR, Barmada MM, Li Y, Zhu D, Maumenee IH: Genetic heterogeneity of dominant optic atrophy, Kjer type: Identification of a second locus on chromosome 18q12.2–12.3. Arch Ophthalmol 1999;117:805–810.
16 Alexander C, Votruba M, Pesch UE, Thiselton DL, Mayer S, Moore A, Rodriguez M, Kellner U, Leo-Kottler B, Auburger G, Bhattacharya SS, Wissinger B: OPA1, encoding a dynamin-related GTPase, is mutated in autosomal dominant optic atrophy linked to chromosome 3q28. Nat Genet 2000;26:211–215.
17 Delettre C, Lenaers G, Griffoin JM, Gigarel N, Lorenzo C, Belenguer P, Pelloquin L, Grosgeorge J, Turc-Carel C, Perret E, Astarie-Dequeker C, Lasquellec L, Arnaud B, Ducommun B, Kaplan J, Hamel CP: Nuclear gene OPA1, encoding a mitochondrial dynamin-related protein, is mutated in dominant optic atrophy. Nat Genet 2000;26:207–210.
18 Shimizu S, Mori N, Kishi M, Sugata H, Tsuda A, Kubota N: A novel mutation of the OPA1 gene in a Japanese family with optic atrophy type 1. Jpn J Ophthalmol 2002;46:336–340.
19 Shimizu S, Mori N, Kishi M, Sugata H, Tsuda A, Kubota N: A novel mutation in the OPA1 gene in a Japanese patient with optic atrophy. Am J Ophthalmol 2003;135:256–257.
20 Yamada T, Hayasaka S, Matsumoto M, Budu, Esa T, Hayasaka Y, Endo M, Nagaki Y, Fujiki K, Murakami A, Kanai A: OPA1 gene mutations in Japanese patients with bilateral optic atrophy unassociated with mitochondrial DNA mutations at nt 11778, 3460, and 14484. Jpn J Ophthalmol 2003;47:409–411.
21 Jones BA, Fangman WL: Mitochondrial DNA maintenance in yeast requires a protein containing a region related to the GTP-binding domain of dynamin. Genes Dev 1992;6:380–389.
22 Pelloquin L, Belenguer P, Menon Y, Ducommun B: Identification of a fission yeast dynamin-related protein involved in mitochondrial DNA maintenance. Biochem Biophys Res Commun 1998;251:720–726.
23 Smirnova E, Shurland DL, Ryazantsev SN, van der Bliek AM: A human dynamin-related protein controls the distribution of mitochondria. J Cell Biol 1998;143:351–358.

24 Pesch UE, Leo-Kottler B, Mayer S, Jurklies B, Kellner U, Apfelstedt-Sylla E, Zrenner E, Alexander C, Wissinger B: OPA1 mutations in patients with autosomal dominant optic atrophy and evidence for semi-dominant inheritance. Hum Mol Genet 2001;10:1359–1368.

25 Pesch UE, Fries JE, Alexander C, Wheeler-Schilling TH, Kohler K, Wissinger B: Spatial and temporal retinal expression of OPA1 involved in autosomal dominant optic atrophy. Invest Ophthalmol Vis Sci 2001;42:S654.

26 Delettre C, Griffoin JM, Kaplan J, Dollfus H, Lorenz B, Faivre L, Lenaers G, Belenguer P, Hamel CP: Mutation spectrum and splicing variants in the OPA1 gene. Hum Genet 2001; 109:584–591.

27 Thiselton DL, Alexander C, Taanman JW, Brooks S, Rosenberg T, Eiberg H, Andreasson S, Van Regemorter N, Munier FL, Moore AT, Bhattacharya SS, Votruba M: A comprehensive survey of mutations in the OPA1 gene in patients with autosomal dominant optic atrophy. Invest Ophthalmol Vis Sci 2002;43:1715–1724.

28 Baris O, Delettre C, Amati-Bonneau P, Surget MO, Charlin JF, Catier A, Derieux L, Guyomard JL, Dollfus H, Jonveaux P, Ayuso C, Maumenee I, Lorenz B, Mohammed S, Tourmen Y, Bonneau D, Malthiery Y, Hamel C, Reynier P: Fourteen novel OPA1 mutations in autosomal dominant optic atrophy including two de novo mutations in sporadic optic atrophy. Hum Mutat 2003;21:656.

29 Nakai K, Sakamoto H: Construction of a novel database containing aberrant splicing mutations of mammalian genes. Gene 1994;141: 171–177.

30 Kitahara K, Kandatsu A, Nishumuta M: An analysis of the results of the Farnsworth-Muncell 100-hue test in acquired blue-yellow defects; in Verriest G (ed): Colour Vision Deficiencies VIII. Dordrecht, Dr W Junk, 1987, pp 157–161.

31 Toomes C, Marchbank NJ, Mackey DA, Craig JE, Newbury-Ecob RA, Bennett CP, Vize CJ, Desai SP, Black GC, Patel N, Teimory M, Markham AF, Inglehearn CF, Churchill AJ: Spectrum, frequency and penetrance of OPA1 mutations in dominant optic atrophy. Hum Mol Genet 2001;10:1369–1378.

32 Antonarakis SE: Recommendations for a nomenclature system for human gene mutations. Nomenclature Working Group. Hum Mutat 1998;11:1–3.

33 den Dunnen JT, Antonarakis SE: Mutation nomenclature extensions and suggestions to describe complex mutations: A discussion. Hum Mutat 2000;15:7–12.

34 Mashima Y, Yamada K, Wakakura M, Kigasawa K, Kudoh J, Shimizu N, Oguchi Y: Spectrum of pathogenic mitochondrial DNA mutations and clinical features in Japanese families with Leber's hereditary optic neuropathy. Curr Eye Res 1998;17:403–408.

35 Verriest G, Van Laethem J, Uvijls A: A new assessment of the normal ranges of the Farnsworth-Munsell 100-hue test scores. Am J Ophthalmol 1982;93:635–642.

36 Mantyjarvi M: Normal test scores in the Farnsworth-Munsell 100 hue test. Doc Ophthalmol 2001;102:73–80.

37 Kitahara K: Individual variations in color vision and its molecular biology. Nippon Ganka Gakkai Zasshi 1998;102:837–849.

38 Krawczak M, Reiss J, Cooper DN: The mutational spectrum of single base-pair substitutions in mRNA splice junctions of human genes: Causes and consequences. Hum Genet 1992;90:41–54.

39 Maquat LE, Carmichael GG: Quality control of mRNA function. Cell 2001;104:173–176.

40 Nagy E, Maquat LE: A rule for termination-codon position within intron-containing genes: When nonsense affects RNA abundance. Trends Biochem Sci 1998;23:198–199.

41 Maquat LE: Nonsense-mediated mRNA decay: Splicing, translation and mRNP dynamics. Nat Rev Mol Cell Biol 2004;5:89–99.

42 Delettre C, Lenaers G, Pelloquin L, Belenguer P, Hamel CP: OPA1 (Kjer type) dominant optic atrophy: A novel mitochondrial disease. Mol Genet Metab 2002;75:97–107.

43 Smith DP: The assessment of acquired dyschromatopsia and clinical investigation of the acquired tritan defect in dominantly inherited juvenile atrophy. Am J Optom Arch Am Acad Optom 1972;49:574–588.

44 Smith DP: Diagnostic criteria in dominantly inherited juvenile optic atrophy. A report of three new families. Am J Optom Arch Am Acad Optom 1972;49:183–200.

45 Brown J Jr, Fingert JH, Taylor CM, Lake M, Sheffield VC, Stone EM: Clinical and genetic analysis of a family affected with dominant optic atrophy (OPA1). Arch Ophthalmol 1997; 115:95–99.

46 Wang L, Dong J, Cull G, Fortune B, Cioffi GA: Varicosities of intraretinal ganglion cell axons in human and nonhuman primates. Invest Ophthalmol Vis Sci 2003;44:2–9.

47 Olichon A, Baricault L, Gas N, Guillou E, Valette A, Belenguer P, Lenaers G: Loss of OPA1 perturbates the mitochondrial inner membrane structure and integrity, leading to cytochrome c release and apoptosis. J Biol Chem 2003;278:7743–7746.

48 Lee YJ, Jeong SY, Karbowski M, Smith CL, Youle RJ: Roles of the mammalian mitochondrial fission and fusion mediators Fis1, Drp1, and Opa1 in apoptosis. Mol Biol Cell 2004;15: 5001–5011.

49 Griparic L, van der Wel NN, Orozco IJ, Peters PJ, van der Bliek AM: Loss of the intermembrane space protein Mgm1/OPA1 induces swelling and localized constrictions along the lengths of mitochondria. J Biol Chem 2004; 279:18792–18798.